IEEE Photonics Journal
An IEEE Photonics Society Publication

Open Access

Investigation and Demonstration of High Speed Full-Optical Hybrid FSO/Fiber Communication System Under Light Sand Storm Condition

Volume 9, Number 1, February 2017

Maged Abdullah Esmail, ***Student Member, IEEE***
Amr Ragheb
Habib Fathallah, ***Senior Member, IEEE***
Mohamed-Slim Alouini, ***Fellow, IEEE***

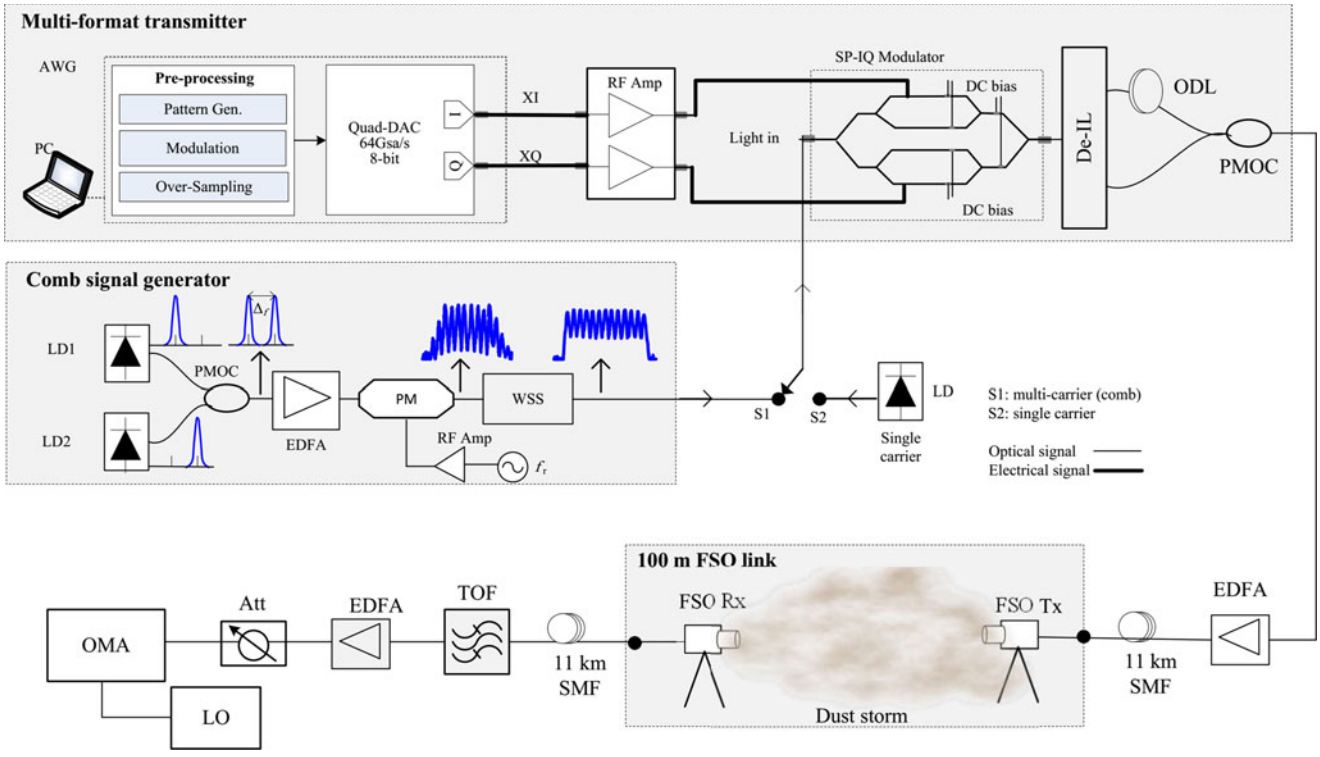

DOI: 10.1109/JPHOT.2016.2641741
1943-0655

Investigation and Demonstration of High Speed Full-Optical Hybrid FSO/Fiber Communication System Under Light Sand Storm Condition

Maged Abdullah Esmail,[1,2] ***Student Member, IEEE*****, Amr Ragheb,**[2]
Habib Fathallah,[1,2,3] ***Senior Member, IEEE*****,**
and Mohamed-Slim Alouini,[4] ***Fellow, IEEE***

[1]Department of Electrical Engineering, King Saud University, Riyadh, 11421, Saudi Arabia
[2]KACST-TIC in Radio Frequency and Photonics for the e-Society, King Saud University, Riyadh, Saudi Arabia
[3]Computer Department, College of Science of Bizerte, University of Carthage, Tunisia
[4]Computer, Electrical, and Mathematical Sciences, and Engineering Division, King Abdullah University of Science and Technology, Thuwal 23955, Saudi Arabia

DOI:10.1109/JPHOT.2016.2641741

Manuscript received November 22, 2016; revised December 10, 2016; accepted December 14, 2016. Date of publication December 19, 2016; date of current version January 6, 2017. This work was supported by the King Abdulaziz City for Science and Technology under Project APR 34-145.

Abstract: In contrast to traditional free space optical (FSO) systems, the new generation is aimed to be transparent to optical fiber where protocols, high signal bandwidths, and high data rates over fiber are all maintained. In this paper, we experimentally demonstrate a high speed outdoor full-optical FSO communication system over 100 m link. We first describe the design of our transmitter, which consists of a comb generator and a flexible multiformat transmitter. Our measurements are performed in arid desert area under a light dust storm. In this environment, we use a 12 subcarrier comb generator, each of which is modulated by a quadrature-amplitude modulation (QAM) signal. We achieved a 1.08 Tbps error free data rate with 3.6 b/s/Hz spectral efficiency. We place long optical fiber rolls in the transmitter side and the receiver side to mimic real FSO deployments. Furthermore, we investigated the effect of receiver misalignment in outdoor conditions and the effect of background noise. We find that full-optical FSO system is sensitive to the misalignment effect. However, the background noise has negligible effect. Finally, we find that solar heating of the transceiver causes collimator deviation, which requires using a cooling unit or auto tracking system.

Index Terms: Free space optical (FSO), super-channel, optical comb generator, hybrid FSO/Fiber network, full-optical FSO.

1. Introduction

Free space optical (FSO) communication technology is viewed as a promising solution for high speed applications when fiber is very expensive, unpractical, or impossible to install. It can deliver high data rate in terabits, with low cost, as an alternative to radio frequency (RF) which is limited in bandwidth and prone to interference [1], [2]. It has unregulated spectrum, i.e., it does not require government licensing for installation. It can be readily deployed in few hours if the establishment of a line-of-sight (LOS) link is possible between the transmitter and receiver sites. Despite these

advantages, the conventional FSO system requires optical/electrical (O/E) and E/O conversion before signal emitting/coupling from/into an optical fiber which limits the system bandwidth to a few gigabits per second. In next generation FSO system, this limitation is overcome when the light signal is directly emitted from the fiber to free space and collimated form free space to the fiber without conversion, then transmitted over a long distance fiber with (or without) a transparent erbium doped fiber amplifier (EDFA), depending on the overall power budget [3]. Therefore, high data rate is transparently transmitted over a sequence of spans composed of fiber and free space segments.

On the other hand, the data rate over fiber has shown a tremendous evolution to satisfy coming/emerging bandwidth/standards requirements (i.e. terabit and beyond). Therefore, researchers are looking for solutions that scale up the network capacity in an efficient way. The traditional wavelength division multiplexing (WDM) networks with fixed spacing between channels leads to a poor spectrum utilization. Recently, the ITU-T defined a new flexible grid termed as super-channel networks which are designed to optimize the channel bandwidth and to allow mixed bit rate and/or mixed modulation formats. [4].

Recently, FSO transmission speed increased rapidly and reached more than 100 Gbps over single carrier thanks to the use of full optical fiber/FSO systems [5]–[9]. Moreover, a demonstration of 1.72 Tbps FSO system has been reported over 10.45 km intended to provide connectivity for rural areas [10]. In [11], we reported a full-optical FSO transmission system in clear weather condition over 11.5 m distance using dual polarization (DP) 16-quadrature-amplitude modulation (QAM) signal. In this paper, we demonstrate a high speed outdoor full-optical FSO transmission system that is transparent to optical single mode fiber (SMF) over 100 m distance. The obtained measurements were taken under a widespread dust storm event having a visibility range of 3 km, i.e., usually referred as light, yet very frequent in desert cities. We studied the effect of background noise caused by sunlight on the system performance. Moreover, we studied the system sensitivity to link misalignment. To simulate real scenarios for FSO deployment, we transmitted the FSO signal through SMF in the transmitter side and in the receiver side. Our measurements indicate that this dust storm introduces 1 dB power loss over 100 m link (i.e., 10 dB/km). In the first setup, we establish error free transmission link at 125 Gbps data rate with 3.7 b/s/Hz efficiency, using 25 Gbaud/32-quadrature amplitude modulation (32-QAM) over a single carrier. Hence, we achieve high spectral efficiency (i.e., almost half that of [6]) but with higher modulation order: 32-QAM. In order to appropriately compare our experimental demonstration, reported in this work, in contrast to the recent FSO experimental demonstrations in literature, the reader is referred to Table 1. In fact, the data rate is not the unique comparison parameter. Table 1 compares the experimental demonstrations of high speed experimental FSO demonstrations along twelve distinct parameters (or criteria) including total data rate (R_t), data rate per carrier (R_c), channel spacing (CS), spectrum efficiency (SE), baud rate (BR), bandwidth (BW), FSO link length (LL), fiber length (FL), environment (ENV, i.e., outdoor or indoor), single or double polarization, modulation scheme, and multiplexing technique.

In our work, we designed and used a super-channel system which has the advantage of eliminating the use of distinct laser for each sub-carrier like in standard WDM systems. Moreover, super-channel system improves the spectral efficiency by eliminating the spectral band gaps between sub-carriers. The designed super-channel system can generate 12 subcarriers with 25 GHz spacing originating from only two laser diodes (LD).

We achieve 1.08 Tbps data rate with 3.6 b/s/Hz spectral efficiency using 18 Gbaud/32-QAM modulation. The other demonstrations in Table 1 use either OOK or QPSK. Our obtained spectral efficiency is better than that of [7–8] and lower than that of the laboratory demonstration in [9] that is based on OAM spaced division multiplexing technology. Note that OAM technique is sensitive to outdoor environment because of turbulence effect that might destroy the orthogonality. Also OAM cannot work with current deployed SMF based optical networks. Furthermore, we demonstrate 22 km fiber/FSO combined link and achieve 864 Gbps data rate with 2.88 b/s/Hz spectral efficiency using 16-QAM modulation.

The remaining of this paper is organized as follows. In Section 2, we describe our experimental setup. In Sections 3 and 4, we analyze the FSO link and the high speed transmission system,

Table 1
Comparison of Single and Multi-Carrier FSO Systems

Reference	[5]	[6]	This work	[7]	[8]	[9]	This Work	This Work
R_t (Gbps)	112	400	125	1280	1600	100,800	864	1080
R_c (Gbps)	–	–	–	40	100	2400	72	90
CS (nm)	–	–	–	0.8	0.8	0.8	0.2	0.2
SE (b/s/Hz)	2*	8*	3.7	0.4	1	24	2.88	3.6
BR (Gbaud)	28	50	25	40	25	50	18	18
BW (GHz)	28*	50*	33.75	3,200	1,600	4,200	300	300
FSO LL (m)	–	120	100	422	80	1	100	100
FL (km)	–	–	22	–	40	–	22	–
Env.	indoor	outdoor	outdoor	outdoor	outdoor	indoor	outdoor	outdoor
Transmission technique	DP/QPSK/ 1λ	SP/QPSK/ 1λ/4 OAM	SP/32-QAM/1λ	SP/OOK/ 32λ -WDM	DP/QPSK/ 16λ -WDM	DP/QPSK/ 42λ -WDM/ 12 OMA	SP/16-QAM/ Super-channel	SP/32-QAM/ Super-channel
Notes	Lab setup	SDM	Our Setup	With repeater	–	SDM/Lab setup	Our Setup	Our Setup

Rt = total data rate, Rc = data rate/carrier, CS = channel spacing, SE = spectrum efficiency, BR = baud rate, FSO LL = FSO link length, FL = fiber length, Env = environment.
*the roll off factor is considered zero so the real spectral efficiency may be less and the bandwidth may be larger.

respectively. In Section 5, we describe the system limitations and provide some insights for open research issues. Finally, we conclude in Section 6.

2. Experimental Setup Description

In this work, we design an optical transmitter with flexibility in both: comb frequency generation and modulation format. We build this system to be reconfigurable and cost-effective. The comb generator has reconfigurable carrier spacing and uses only two LDs instead of a dedicated LD for each carrier. The multi-format transmitter is reconfigurable with capability to generate most of common coherent optical modulation formats at variable baud rates. Furthermore, the FSO link is transparent to fiber where optical/electrical conversion is not needed. Hence, data rate in terabit order can be achieved.

2.1. Super-Channel Comb Generator

Pulsed mode-locked laser (MLL) source, array of LD sources, and electro-optic (EO) modulators are among the main approaches to exploit comb circuits [12–13]. For our experimental setup, we build a flexible/reconfigurable frequency comb source (FCS) that is based on the integration of only two laser sources, with pre-defined spacing, into a single electro-optic phase modulator. The developed FCS compromises between the circuit complexity and the number of generated comb lines in order to achieve terabit transmission over free space optical (FSO) channel.

Our designed comb generator is shown in Fig. 1(a). The goal here is to generate a maximum number of subcarriers with flat gain. Two narrow linewidths (<10 kHz) distributed feedback laser diodes (DFB-LDs) are used at 1550.216 nm and 1551.216 nm wavelengths. Then a polarization

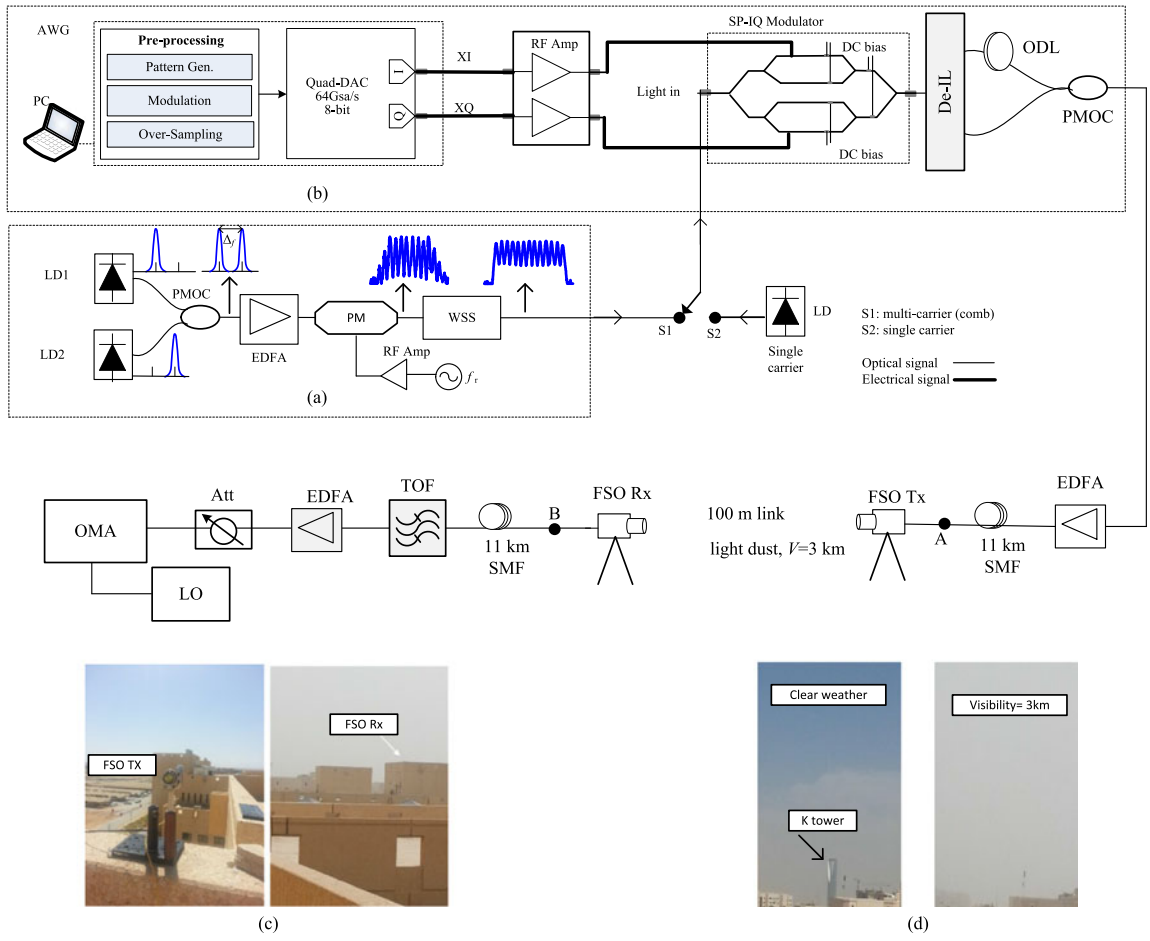

Fig. 1. Experimental setup for full-optical hybrid FSO system. (a) Comb generator using two LDs and one PM. (b) Flexible multi-format transmission system. Shaded boxes mean these devices are not used in single carrier setup. (c) FSO link on the building roof. (d) Effect of dust storm (right) and clear weather (left). AWG: arbitrary waveform generator, DAC: digital-to-analog converter, RF: radio frequency, SP: single polarization, ODL: optical delay line, PMOC: polarization maintaining optical coupler, EDFA: erbium doped fiber amplifier, SMF: single mode fiber, TOF: tunable optical filter, LO: local oscillator, OMA: optical modulation analyzer, LD: laser diode, PM: phase modulator, WSS: wave select shaper. Gray shaded boxes are not used for single carrier demonstration.

maintaining 3 dB optical coupler (PMOC) is used to combine both lasers' lights. An EDFA is used to boost the signals before modulating them by the phase modulator (PM). In the PM, an RF signal with 25 GHz (0.2 nm) is used. The PM output signal can be expressed as

$$E_{PM} = 2E_o \cos(\pi \Delta f\, t) \sum_{k=-\infty}^{\infty} J_k(\pi R) \exp\left(j2\pi(kf_r + f_1 + \Delta f/2)t\right) \quad (1)$$

where E_o is the field amplitude, f_r is the RF signal frequency, f_1 and $f_2 = f_1 + \Delta f$ are the LD's frequencies, Δf is the frequency spacing between LDs, R is the ratio of the RF signal amplitude to the half-wave voltage of the PM, and $J_k(\pi R)$ is the first kind k^{th} Bessel order function which determines the amplitude of the k^{th} harmonic subcarrier. The parameter R controls the number of generated carriers. As R increases, the transferred power to the higher order subcarriers increases. Unfortunately, because the electrical amplifier power is limited, the amplitude of RF drive signal is limited in practical operation. In our setup, we applied 5 dBm RF signal enabling to generate 12 subcarriers with 0.2 nm wavelength spacing and 300 GHz total bandwidth. Then a wave selector shaper (WSS) (Finisar WaveShaper 4000S) is used for fine gain equalization.

Note that the spacing between both LDs should be an integer multiple (n) of the RF signal frequency, i.e., $\Delta f = n \times f_r$, to avoid beat lines to appear between the generated subcarriers. In our setup, $n = 5$.

2.2. Multi-format Transmitter

Fig. 1(b) shows our flexible multi-format transmitter prototype with capability to generate SP-IQ signal [14]. The Keysight M8195 arbitrary waveform generator (AWG) includes a configuration software and a quadruple digital-to-analog convertor (DAC). The targeted modulation format and the oversampling factor is controlled by the configuration prototype software. A two-channel multi-level signal is generated by the 64 GSa/s, 8 bits DAC. The DAC's output signals feed a two channels' amplifier which has a flat 3-dB bandwidth of 30 GHz, simultaneously providing 20 dB gain for each channel. The driving signals are lunched to the two RF inputs of the SP-IQ modulator in order to modulate the drive laser source. The IQ modulator consists of three sub-modulators as shown in Fig. 1(b). The first two sub-modulators generate the I and Q signals, while the third one puts them in quadrature form (90° phase shift). For each modulator, a bias voltage is used to set the operating point. The IQ modulator enables up to 32 Gbaud with π-phase shift voltage of 3.5 V. To maintain signal stability, automatic bias controller (ABC) is used to control the bias voltage of the modulator.

After comb signal generation, the signal is modulated by the multi-format transmitter with 16-QAM and 32-QAM modulation schemes at different baud rates. Since all carriers are modulated using the same data, a mux/de-mux device with delay line is needed to decorrelate the adjacent channels. In this setup, we used 25 GHz optical de-interleaver as a de-multiplexer to separate the odd and even channels. Then we used an optical delay line (ODL) to de-correlate them. After de-correlation, we multiplex the channels using PMOC, amplify them and then directly transmit them over the FSO link or over 11 km SMF to simulate real scenarios of hybrid FSO/Fiber network. The used SMF is a G.652.B ultra-low-loss fiber type having 0.181 dB/km attenuation loss and less than 18 ps/nm.km dispersion coefficient at 1550 nm. Note that for single carrier transmission, the shaded boxes in Fig. 1 correspond to the devices that are not used.

2.3. Full-Optical FSO System

The complete experimental setup is shown in Fig. 1. The FSO link with 100 m distance was installed on the roof of our department building. The transmitted signal from the output of the arbitrary format transmitter is sent to the FSO transceiver using SMF. Recall that we mounted full-optical FSO link where E/O and O/E conversion is not required. This makes the FSO link transparent to fiber and capable of transmitting high speed data in Terabits. The FSO transceivers use doublet lenses that are pre-aligned at 1550 nm wavelength. The output beam diameter is 7 mm with 0.016° (279 μrad) full-angle beam divergence. A visible light source at 520 nm is used for initial alignment. Fine tuning is then applied in order to make precise alignment. Note that all active devices (including laser, receiver, and amplifiers) are placed indoor, i.e., outdoor FSO link is connected through SMF in the transmitting and receiving ends. Fig. 1(c) shows the FSO transmitter and receiver on the building roof.

The collimated beam in FSO receiver side is focused to a SMF which is connected to the laboratory. This SMF in the receiver side is introduced to mimic real scenarios when optical fiber deployment is difficult due to physical obstacles (such as rivers, railways, highways, private territories, etc.) [15]. In this case, FSO can work as an interconnection between fiber segments.

The received signal can be connected directly to a tunable optical filter (TOF) (Santec OTF-350) to select the desired wavelength or it can be first transmitted over an 11 km SMF. The TOF's 3 dB bandwidth is adjusted to 25 GHz (0.2 nm) which has side lobe suppression of 50 dB. An EDFA is used to boost the received signal and compensate for FSO and filter attenuation. Then, an optical attenuator is used before applying the signal to Keysight N4391A optical modulation analyzer (OMA) with 80 GSa/s sampling rate and 64 GHz bandwidth for data analysis.

3. Full-Optical Link Analysis

We first transmit a continuous wave at 1550 nm wavelength over the FSO system to measure the FSO link power loss. The measured SMF-to-SMF power loss between A and B points in Fig. 1 is 16 dB over 100 m link. This includes the optical and coupling loss and the geometrical loss due to beam spread. The laser beam generated by a LD is assumed to have ideal Gaussian profile with circularly symmetrical intensity distribution. The theoretical geometrical loss due to beam divergence for Gaussian beam is given by [16]

$$L_G = 10 \log \left\{ 1 - \exp \left(-2 \left[\frac{r_{Rx}}{l \tan(\theta/2)} \right]^2 \right) \right\} \tag{2}$$

where $r_{Rx} = 0.35$ cm is the receiver aperture radius. The link length $l = 100$ m, and the full angle beam divergence $\theta = 279\,\mu$rad. Using (2), the geometrical loss is found to be 9.3 dB. This loss can be reduced using larger collimators (unfortunately not available at the time of the experiment). The remaining 6.7 dB is due to light optical loss of the lenses and collimation loss. As compared to traditional FSO that use a photodetector with few millimeters diameter, the full-optical FSO collimates the light to SMF that has about 9 μm diameter. Therefore, light coupling into SMF is very difficult, and requires precise tuning of X-Y lens position, as well as tilt/tilt adjustment. As the transmission distance increases, this difficulty substantially increases. Although, in our setup, we have used precise alignment tools to adjust the link and reduce the loss, the obtained loss calls for using more precise tools or automatic tracking system.

Fig. 2(a) shows the received power as a function of receiver misalignment (displacement from the beam center). We notice that the amount of power loss depends on the amount of misalignment in x-axis direction, and y-axis direction. This power loss increases as the misalignment increases. For example, the power loss due to 0.5 cm misalignment in x-direction is 2 dB which increases four times at 1.5 cm misalignment. The results in Fig. 2(a) show that full-optical FSO system is very sensitive to misalignment. Note that the calculated received beam spot size is 3.5 cm which is five times wider than the collimator aperture size as shown in Fig. 2(b). However, the collimator in the receiver side loses much power due to misalignment even if it is still in the spot range. Note that in Fig. 2(a) we showed the effect of receiver misalignment in x or y directions. In reality, the misalignment can be in both directions and also can be angular which results in higher power loss. This high sensitivity calls for the use of automatic tracking system in the transceiver.

In Fig. 3, we investigate the effect of the background noise (also called ambient noise), on the FSO signal in full-optical FSO system. This noise arises from sunlight that is either direct, scattered by aerosols in the atmosphere, or reflected from the objects surroundings of the receiver. We measured the receiver noise during the night when there is no background noise, and compared it to the noise measurements at the morning and around noon. We see that all measurements show very close noise variances of 3.08×10^{-16}, 2.87×10^{-16}, and 3.07×10^{-16} corresponding to night, morning, and noon measurements, respectively. This shows that the background noise has negligible effect on the full-optical FSO link. The is mainly due to the following aspects: 1) The angle of view of the collimation setup at the receiver is very low, and hence, it does not gather much of the sunlight; 2) the collimator of the receiver operates at the 1550 nm communication C band and does not collimate other bands where the sunlight has its maximum power density; 3) the used fiber has a cutoff wavelength at 1260 nm so it rejects background noise lower than this wavelength; and 4) the photodetector used in the communication setup is an InGaAsP that is optimized to work also in C band and has very low responsivity at the sunlight bands. These factors together lead to negligible background noise effect on the full-optical FSO system. This is not the case in traditional FSO links that operate in spectral bands where sunlight has high power density and also has large angle of view. Therefore, they are more affected by background noise, which reduces the signal-to-noise ratio and the effective receiver sensitivity [2].

Because the FSO link is installed outdoor, it is subject to solar heating effect. Although the FSO link is all passive (i.e., no electronics and consequently no cooling is required), the precise alignment tools and mounts that are used to adjust the link are subject to thermal expansion. These mounts

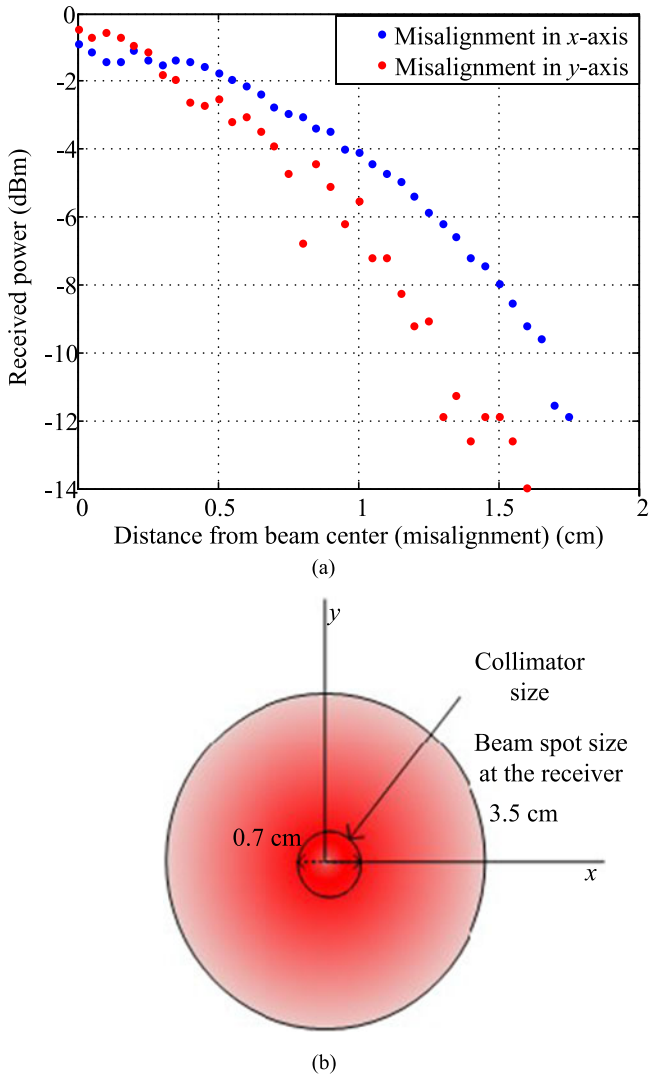

Fig. 2. (a) Misalignment effect on the received signal and (b) received spot size as compared to the collimator aperture size.

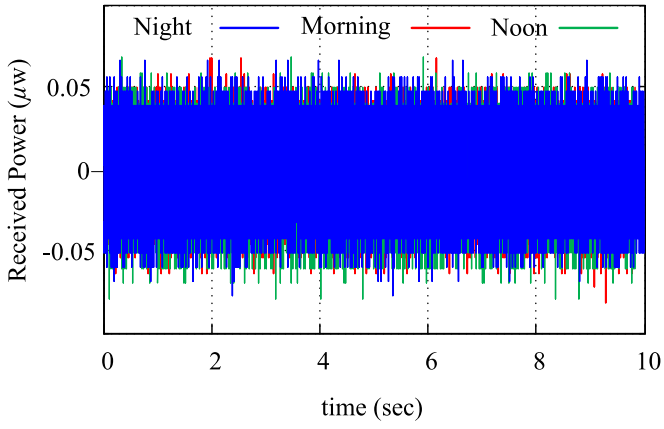

Fig. 3. Investigation of solar radiation effect on the received signal. Measurements are taken at night, morning, and noon.

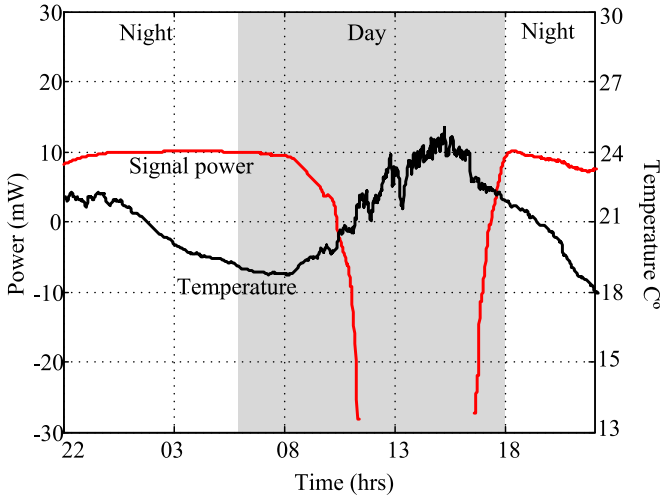

Fig. 4. Effect of solar heating on the link alignment.

have high resolution (11 mrad/rev) and are sensitive to temperature change. The collimators are mounted on these mechanical devices, leading the whole collimation and hence the link stability to be sensitive to temperature variation. This introduces a serious misalignment problem that might lead to link drop. Figure 4 shows the effect on temperature change which is related to solar heating. At night, the temperature is low and the power is almost constant. However, when the sun arises, the solar heating effect increases with time leading to signal loss. To solve this issue, the FSO link needs to be installed behind window so the effect of solar heating is eliminated. Another option is using air sealed-enclosure or automatic tracking system.

4. High Speed System Performance Analysis

The measurements were taken in light (blowing widespread) dust storm in Riyadh city (March 27, 2016). Fig. 1(d) shows the weather with light dust storm and without dust in clear weather. The visibility range reported by the meteorological station in the National Airport was 3 km. In addition, we measured some weather parameters using a weather station located at the FSO link installation site. The reported temperature, average wind speed, and humidity are 31 C°, 3 m/s, and 16%, respectively. These measurements' values show low effect on the system performance.

4.1. Single Carrier FSO System Results

We start our experimental work by transmitting data over single carrier at 1550.216 nm. The carrier is modulated by SP-16-QAM and SP-32-QAM signals at 25 Gbaud with 0.35 raised cosine roll off factor. The maximum achieved data rate is 125 Gbps for 32-QAM signal with 3.7 b/s/Hz spectral efficiency. Fig. 5 shows the obtained bit error rate (BER) versus the optical received power. First, we have noticed about 1 dB degradation in system performance when the visibility reduces from clear weather down to 3 km, due to the blowing dust storm. This value of attenuation is close to the predicted value by dust attenuation prediction model in [17] which is 1.6 dB over 100 m link length.

Next, the performance of the 16-QAM signal is compared with that of 32-QAM signal for the same baud rate over 100 m FSO link. We notice more than one order of magnitude degradation due to using higher modulation order. Moreover, we investigated the system performance when 22 km SMF (11 km in each side of the link) is used to simulate real scenarios of hybrid FSO/fiber network applications. The results show clearly more degradation in system performance compared to only FSO link. The degradation is more than one order of magnitude between 16-QAM and 32-QAM signal at the same baud rate. However, the system is still able to achieve error free transmission

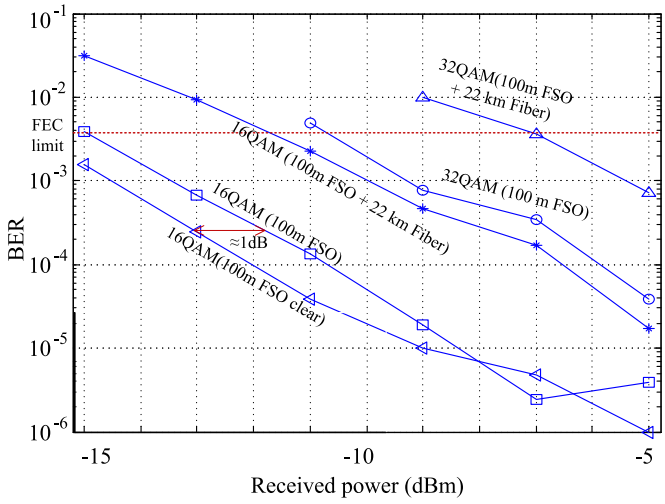

Fig. 5. BER versus the received optical power for single carrier signal at 25 Gbaud.

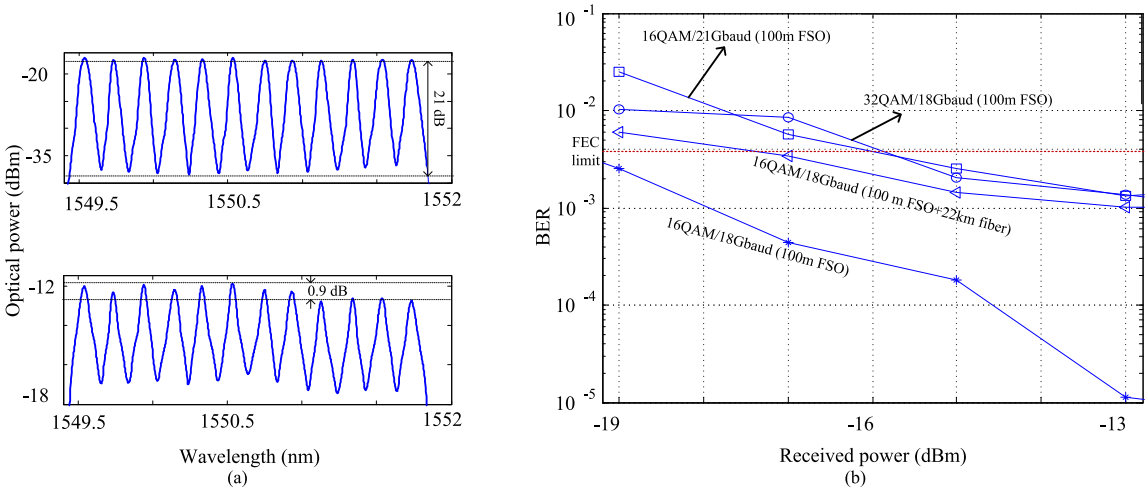

Fig. 6. (a) Comb signal power spectrum (unmodulated (top), modulated (bottom)) and (b) BER versus the optical received power for comb signal.

(i.e., BER lower than the forward error correction (FEC) limit: BER $= 3.8 \times 10^{-3}$). Note that the obtained BER is inferred from the error vector magnitude (EVM) under the assumption that the noise is Gaussian [18].

4.2. Super-channel FSO System Results

Fig. 6(a) shows the comb signal with 12 subcarriers spaced by 0.2 nm (25 GHz). The total bandwidth is $\sim$ 300 GHz or 2.4 nm. Each subcarrier is modulated by 16-QAM or 32-QAM signals. The power spectrum of the super-channel signal is shown in Fig. 6(a). The top figure shows the power spectrum after WSS while the modulated signal spectrum is shown in the bottom figure. We notice that the generated comb signal has a flat spectrum with 21 dB carrier-to-noise ratio. The spectrum of the modulated signal is almost flat with at most 0.9 dB difference in amplitude. The maximum transmitted baud rate is 21 Gbaud with 0.1 roll off factor (i.e. 23.1 GHz); therefore, there is at least 3.8 GHz guard band between any adjacent channels which reduces the interference effect. The remaining part of inter-channel interference can be rejected using signal processing in the OMA or receiver.

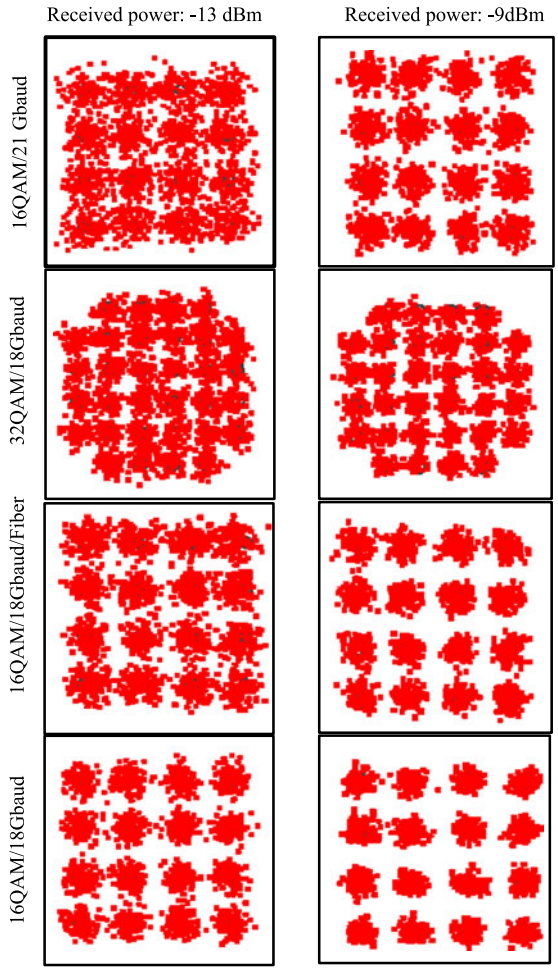

Fig. 7. Constellation diagram of the received signal at different optical received power values.

In the receiver side, we set the local oscillator (LO) to demodulate one of the 12 subcarriers. Fig. 6(b) shows the BER versus the received power for the 16-QAM and 32-QAM signal with 0.1 roll off factor, under low visibility weather. We notice that for the same baud rate (18 Gbaud), the 16-QAM signal has lower BER than the 32-QAM signal with more than one order of magnitude. Moreover, the 16-QAM signal with 21 Gbaud and the 32-QAM signal with 18 Gbaud have close performance. When SMF is used, the system performance degraded for the 16-QAM signal by about one order of magnitude.

The maximum achieved baud rate is 21 Gbaud for the 16 QAM signal which corresponds to 1.008 Tbps. Moreover, we achieved 32-QAM modulation order at 18 Gbaud rate which corresponds to 1.08 Tbps. For the latter data rate, we achieved 3.6 b/s/Hz spectral efficiency with 25 GHz spacing and 0.1 raised cosine roll off factor. When SMF is used in the transmitter side and also the receiver side (22 km SMF length), the achieved data rate drops to 864 Gbps due to signal attenuation dispersion introduced by fiber.

In Fig. 7, we show the constellation diagram for different FSO signals at two different received optical power. We see that for high QAM signal and low received power, the constellation is degraded showing high BER. As the received power improved or the QAM signal format decreases, the constellation improves, reflecting lower BER.

5. Challenges and Future Work

In this section, we discuss the different practical/experimental challenges that faced in this work and propose solutions to overcome these limitations and improve the experimental demonstration reported in this paper. These limitations concerned in the comb generator, multi-format transmitter, outdoor FSO components, and the weather conditions that limit achieving higher data rate. The generated signal by the comb consists of 12 subcarriers which allowed us to achieve one terabit data rate. However, using higher power RF amplifier can increase the number of subcarriers and this will in turn increase the amount of transmission bandwidth.

The used multi-format transmitter is capable of generating high modulation orders up to 256 QAM signal which in turn allows transmitting high data rate over each single carrier. However, the electronics of the multi-format transmitter have limited bandwidth which limits the maximum achievable baud rate.

In our setup, the outdoor FSO link is built using collimators that have small size apertures with 7 mm output beam diameter. This caused about 9.3 dB power loss. Using larger size apertures can enhance the power budget and improve the system performance. For example, if the aperture size increases up to 5 cm, the geometrical loss dramatically drops to near 0 dB. Moreover, using lenses with small full-angle beam divergence can improve the power budget. For example, if the full-angle beam divergence is reduces to 100 μrad, the geometrical loss drops to 2 dB.

The outdoor atmospheric condition has a negative impact on the FSO system. During our measurements, the light dust storm introduced 1 dB power loss. Under moderate to thick dust, the signal attenuation quickly increases and the data rate reduces significantly. Similarly but less effective, other weather conditions such as fog and rain can cause degradation in system performance. Although we used precise alignment tools to align the link, the power loss due to misalignment was 6.7 dB. Therefore, using auto-tracking system can reduce such loss. In addition, the auto-tracking system can reduce the solar heating effect.

As a future work, developing and testing a fast automatic tracking system with efficient algorithms that can automatically keep the link in its initial condition will add an important value to such systems. Moreover, applying some mitigation techniques such as MIMO and aperture averaging can enhance the system performance [19]. Furthermore, integrating the full-optical FSO setup with milimeter wave (MMW) system can improve the system reliability in harsh environments [20].

6. Conclusion

In this paper, we demonstrated high speed full-optical FSO and hybrid Fiber/FSO link with reconfigurable/flexible transmitter. We achieved 1.08 Tbps data rate using high modulation format (32-QAM) with 18 Gbaud symbol rate. High spectral efficiency equals 3.6 b/s/Hz was obtained. The achieved BER was under the FEC limit; hence, error free transmission is possible using proper coding. Moreover, we studied the system performance using optical fiber segments in the transmitter and receiver side. The background noise due to sunlight is found to have negligible effect on this FSO system. However, our investigation of receiver misalignment shows that this system is sensitive to misalignment which requires using automatic tracking system to overcome it.

References

[1] Y. Li, N. Pappas, V. Angelakis, M. Pióro, and D. Yuan, "Optimization of free space optical wireless network for cellular backhauling," *IEEE J. Sel. Areas Commun.*, vol. 33, no. 9, pp. 1841–1854, Sep. 2015.
[2] M. A. Khalighi and M. Uysal, "Survey on free space optical communication: A communication theory perspective," *IEEE Commun. Surveys Tuts.*, vol. 16, no. 4, pp. 2231–2258, Oct.–Dec. 2014.
[3] M. Matsumoto, "Next generation free-space optical system by system design optimization and performance enhancement," in *Proc. Progress Electromagn. Res. Symp.*, Kuala Lumpur, Malaysia, Mar. 2012, pp. 27–30.
[4] Spectral Grids for WDM Applications: DWDM Frequency Grid, ITU-T Standard G.694.1, 2012.
[5] N. Cvijetic, D. Qian, J. Yu, Y.-K. Huang, and T. Wang, "100 Gb/s per-channel free-space optical transmission with coherent detection and MIMO processing," in *Proc. 35th Eur. Conf. Opt. Commun.*, Vienna, Austria, Sep. 2009, pp. 1–2.

[6] Y. Ren *et al.*, "400-Gbit/s free space optical communications link over 120-meter using multiplexing of 4 collocated orbital-angular-momentum beams," in *Proc. Opt. Fiber Commun. Conf.*, Los Angeles, CA, USA, Mar. 2015, pp. 1–3.
[7] E. Ciaramella *et al.*, "1.28 Terabit/s (32x40 Gbit/s) WDM transmission system for free space optical communications," *IEEE J. Sel. Areas Commun.*, vol. 27, no. 9, pp. 1639–1645, Dec. 2009.
[8] G. Parca, A. Shahpari, V. Carrozzo, G. M. T. Beleffi, and A. L. Teixeira, "Optical wireless transmission at 1.6-Tbit/s (16 $\times$ 100 Gbit/s) for next-generation convergent urban infrastructures," *Opt. Eng.*, vol. 52, no. 11, pp. 116102-1–116102-5, Nov. 2013.
[9] H. Huang *et al.*, "100 Tbit/s free-space data link enabled by three-dimensional multiplexing of orbital angular momentum, polarization, and wavelength," *Opt. Lett.*, vol. 39, no. 2, pp. 197–200, Jan. 2014.
[10] German Aerospace Center (DLR), "World record in free-space optical communications," Nov. 2016. [online]. Available: http://www.dlr.de/dlr/en/desktopdefault.aspx/tabid-10081/151_read-19914#/gallery/24870
[11] M. A. Esmail, A. Ragheb, H. Fathallah, and M. S. Alouini, "Experimental demonstration of outdoor 2.2 Tbps super-channel FSO transmission system," in *Proc. IEEE Int. Conf. Commun. Workshops*, Kuala Lumpur, Malaysia, 2016, pp. 169–174.
[12] P. M. Anandarajah *et al.*, "Flexible optical comb source for super channel systems," in *Proc. Opt. Fiber Commun. Conf. Expo. Nat. Fiber Opt. Eng. Conf.*, Anaheim, CA, USA, Mar. 2013, pp. 1–3.
[13] X. Liu, S. Chandrasekhar, P. J. Winzer, R. W. Tkach, and A. R. Chraplyvy, "406.6-Gb/s PDM-BPSK superchannel transmission over 12,800-km TWRS fiber via nonlinear noise squeezing," in *Proc. Opt. Fiber Commun. Conf. Expo. Nat. Fiber Opt. Eng. Conf.*, Anaheim, CA, USA, Mar. 2013, pp. 1–3.
[14] A. M. Ragheb *et al.*, "Up to 64 QAM/32 Gbaud flexible dual polarization transmitter for future elastic optical networks," *Opt. Eng.*, vol. 52, no. 11, pp. 115102–115102, Nov. 2013.
[15] H. Willebrand and B. S. Ghuman, *Free Space Optics: Enabling Optical Connectivity in Today's Networks*. Indianapolis, IN, USA: SAMS, 2002.
[16] J. Poliak, P. Pezzeiy, E. Leitgeby, and O. Wilfert, "Analytical expression of FSO link misalignments considering Gaussian beam," in *Proc. 18th Eur. Conf. Netw. Opt. Commun. 8th Conf. Opt. Cabling Infrastruct.*, Graz, Austria, 2013, pp. 99–104.
[17] M. A. Esmail, H. Fathallah, and M. S. Alouini, "An experimental study of FSO link performance in desert environment," *IEEE Commun. Lett.*, vol. 20, no. 9, pp. 1888–1891, Sep. 2016.
[18] R. Schmogrow *et al.*, "Error vector magnitude as a performance measure for advanced modulation formats," *IEEE Photon. Technol. Lett.*, vol. 24, no. 1, pp. 61–63, Jan. 2012.
[19] R. Tian-Peng, C. Yuen, Y. L. Guan, and T. Ge-Shi, "High-order intensity modulations for OSTBC in free-space optical MIMO communications," *IEEE Wireless Commun. Lett.*, vol. 2, no. 6, pp. 607–610, Dec. 2013.
[20] M. Usman, H. C. Yang, and M. S. Alouini, "Practical switching-based hybrid FSO/RF transmission and its performance analysis," *IEEE Photon. J.*, vol. 6, no. 5, pp. 1–13, Oct. 2014.